HHS Public Access

Author manuscript

Mol Neurobiol. Author manuscript; available in PMC 2017 July 01.

Published in final edited form as:

Mol Neurobiol. 2017 July ; 54(5): 3119–3130. doi:10.1007/s12035-016-9884-4.

Inflammation in Lafora Disease: evolution with disease progression in laforin and malin knock-out mouse models

Irene López-González, MSc[1,#], **Rosa Viana, PhD**[4,#], **Pascual Sanz, PhD**[4,5,CA], and **Isidre Ferrer, MD, PhD**[1,2,3,CA]

[1]Institute of Neuropathology, Bellvitge University Hospital, Idibell, Hospitalet de Llobregat, Barcelona, Spain

[2]University of Barcelona, Hospitalet de Llobregat, Barcelona, Spain

[3]CIBERNED (Centro de Investigación Biomédica en Red de Enfermedades Neurodegenerativas), Ministry of Science and Innovation, Institute Carlos III, Spain

[4]Instituto de Biomedicina de Valencia, Consejo Superior de Investigaciones Científicas; Valencia, Spain

[5]CIBERER (Centro de Investigación Biomédica en Red de Enfermedades Raras), Institute Carlos III, Spain

Abstract

Lafora progressive myoclonus epilepsy (Lafora disease, LD) is a fatal rare autosomal recessive neurodegenerative disorder characterized by the accumulation of insoluble ubiquitinated polyglucosan inclusions in the cytoplasm of neurons, which is most commonly associated with mutations in two genes: *EPM2A*, encoding the glucan phosphatase laforin, and *EPM2B*, encoding the E3-ubiquitin ligase malin. The present study analyzes possible inflammatory responses in the mouse lines *Epm2a*$^{-/-}$ (laforin knock-out) and *Epm2b*$^{-/-}$ (malin knock-out) with disease progression. Increased numbers of reactive astrocytes (expressing the GFAP marker) and microglia (expressing the Iba1 marker) together with increased expression of genes encoding cytokines and mediators of the inflammatory response occur in both mouse lines although with marked genotype differences. *C3ar1* and *CxCl10* mRNAs are significantly increased in *Epm2a*$^{-/-}$ mice aged 12 months when compared with age-matched controls, whereas *C3ar1*, *C4b, Ccl4*, *CxCl10*, *Il1b*, *Il6*, *Tnfα* and *Il10ra* mRNAs are significantly up-regulated in *Epm2b*$^{-/-}$ at the same age. This is accompanied by increased protein levels of IL1-β, IL6, TNFα and Cox2 particularly in *Epm2b*$^{-/-}$ mice. The severity of inflammatory changes correlates with more severe clinical symptoms previously described in *Epm2b*$^{-/-}$ mice. These findings show for the first time

[CA]Corresponding authors: Prof. I. Ferrer, Institut de Neuropatologia, Servei Anatomia Patologica, Hospital Universitari de Bellvitge, Carrer Feixa Llarga sn, 08907 Hospitalet de Llobregat, Spain, Phone number: +34 93 260 7452; Fax number: +34 93 260 7503, 8082ifa@gmail.com; Prof. P. Sanz, Instituto de Biomedicina de Valencia, Consejo Superior de Investigaciones Científicas, Jaime Roig 11, 46010 Valencia, Spain. Phone number: +34 96 339 1779; Fax number: +34 96 369 0800; sanz@ibv.csic.es.
[#]These authors contributed equally to this work.

Financial disclosure and conflict of interests
No relevant data.

Statement of author contributions
I.L-G carried out the analysis of gene and protein expression; R.V. did the immunohistochemical study; P.S. and I.F. designed and supervised the work. All authors were involved in writing the paper and had final approval of the submitted and published version.

increased innate inflammatory responses in a neurodegenerative disease with polyglucosan intraneuronal deposits which increase with disease progression, in a way similar to what is seen in neurodegenerative diseases with abnormal protein aggregates. These findings also point to the possibility of using anti-inflammatory agents to mitigate the degenerative process in LD.

Keywords

Lafora disease; polyglucosan; inflammation; cytokines; chemokines; microglia

Introduction

Lafora progressive myoclonus epilepsy (Lafora disease, LD, OMIM 254780, ORPHA501) is a fatal rare autosomal recessive neurodegenerative disorder, which usually occurs during childhood. It is characterized by generalized tonic-clonic seizures, myoclonus, absences, drop attacks and visual seizures. As the disease progresses, patients present a rapid progressive dementia concomitant with an amplification of seizures, leading to death within a decade after the first symptoms [1, 2]. The hallmark of the disease is the accumulation of insoluble polyglucosan inclusions, called Lafora bodies (LBs), in the cytoplasm of neurons and other cells in peripheral tissues. In the vast majority of patients LD has been associated with mutations in two genes: *EPM2A*, encoding the glucan phosphatase laforin, and *EPM2B*, encoding the E3-ubiquitin ligase malin. Although laforin and malin may have independent functions, it has been shown that they form a functional complex in which laforin acts as scaffold and recruits specific substrates to be ubiquitinated by malin. It has also been demonstrated that laforin and malin regulate glycogen synthesis, either by affecting the activity of proteins involved in this process [3–6] or by laforin's acting as a glycogen phosphatase and thus being able to dephosphorylate complex glucans [7–9]. This would explain why the absence of laforin or malin leads to aberrant glycogen accumulation in neurons in the form of LBs, which are glycogen-like inclusions with a greater degree of phosphorylation and less branching than normal glycogen. Hence LBs are largely insoluble.

Recent work has demonstrated that neuronal death in LD can be influenced not only by the accumulation of LBs but also by impairment in mechanisms related to protein clearance. For instance, endoplasmic reticulum stress is significantly increased in mouse models of LD [10–13], and molecular interactions between laforin, malin and the chaperone and proteasome systems [14, 15] have been described. This body of evidence points to a critical dysregulation of cellular protein homeostasis in LD that goes beyond alterations in glycogen metabolism regulation. In this sense, our previous work with mouse models of LD such as *Epm2a*$^{-/-}$ [16] and *Epm2b*$^{-/-}$ [17] revealed impairment of autophagy and defects in the ubiquitin-proteasome system [12, 18] which correlated with neurological and behavioral abnormalities. We have also described increased oxidative stress and impaired antioxidant response in LD cellular and mouse models [19], thus suggesting that oxidative stress is a new hallmark in the pathogenesis of LD [20]. These results are in agreement with the hypothesis that defects in autophagy and protein clearance are related with an increase in reactive oxygen species (ROS) production and consequent oxidative stress [21–24]. It is feasible that alterations in protein homeostasis and oxidative stress could underlie the

appearance of reactive astrogliosis observed in different brain areas of malin knock-out (*Epm2b*$^{-/-}$) mice [25, 26]. Microglia activation and neuroinflammatory responses are currently observed in most neurodegenerative diseases and they are determinants in the pathogenesis of these processes [27–30]. However, very little is known about inflammatory responses and most particularly about gene modulation of cytokines and mediators of the immune response along with disease progression in LD. The present study is focused on possible inflammatory responses in the brain of laforin knock-out (*Epm2a*$^{-/-}$) and malin knock-out (*Epm2b*$^{-/-}$) mice to learn whether inflammation plays a role in the pathogenesis of LD, in the same way that inflammation has functional implications in the pathogenesis of neurodegenerative diseases with abnormal protein aggregates.

Material and methods

Ethical statement, animal care, mice and husbandry

This study was carried out in strict accordance with the recommendations in the Guide for the Care and Use of Laboratory Animals of the Consejo Superior de Investigaciones Cientificas (CSIC, Spain). All mouse procedures were approved by the animal committee of the Instituto de Biomedicina de Valencia-CSIC [Permit Number: INTRA12 (IBV-4)]. All efforts were made to minimize animal suffering. To eliminate the effect of differences in the genetic background of the animals, we backcrossed *Epm2a*$^{-/-}$ and *Epm2b*$^{-/-}$ mice (with a mixed background 129sv:C57BL/6) as previously described [16, 17, 31]) with control C57BL/6JRccHsd mice obtained from Harlan laboratories (Barcelona, Spain) ten times to obtain homozygous *Epm2a*$^{-/-}$ and *Epm2b*$^{-/-}$ in a pure background. Mice were maintained in the IBV-CSIC facility on a 12/12 light/dark cycle under constant temperature (23°C) with food and water provided *ad libitum.*

Male mice of 16 days, 3 and 12 months of age were sacrificed by cervical dislocation. Brain was recovered and the two hemispheres separated, one conserved at −80°C for processing for western blot and qPCR analyses, and the other fixed in 4% paraformaldehyde in phosphate buffer saline (PBS) for immunohistochemical analyses.

Immunohistochemical analyses

Dehydrated tissues from at least three independent mice per group were embedded in paraffin and sectioned at 4μm. Some sections were stained with periodic acid Schiff (PAS). Other sections were de-waxed, rehydrated, and warmed at 95°C for 30 min in 10 mM citrate buffer for antigen retrieval. Sections were blocked in blocking buffer (1% bovine serum albumin; 5% fetal bovine serum in PBS) and incubated overnight at 4°C with the appropriate primary antibody diluted in blocking buffer: anti-GFAP (diluted 1/300; Sigma ref. G3893, Saint Louis, MO, USA), Iba-1 (diluted 1/200; Waco ref. 019-19741, Richmond, VA, USA) and anti-Cox2 (diluted 1/250; Cayman Chemicals ref. 160107, Ann Arbor, MI, USA). After three washes of 10 min in PBS, sections were incubated for 1 h at room temperature with the corresponding biotin-conjugated anti-rabbit or anti-mouse secondary antibody (Jackson ImmunoResearch, West Grove, PA, USA) diluted in blocking buffer, washed three times with PBS for 5 min and visualized with the Avidin–Biotin Complex (ABC) (Vectastain Elite ABC kit, Vector Laboratories, Burlingame, CA, USA) using diaminobenzidine as

chromogenic substrate for peroxidase (Peroxidase substrate kit DAB; Vector Laboratories, Burlingame, CA, USA). Sections were slightly counterstained with hematoxylin (Sigma, Madrid, Spain), dehydrated, and mounted in DPX (Merck, Germany). Images were acquired by light microscopy (Leica DM RXA2, Leica Microsystems, Wetzlar, Germany) and analyzed with Image J software (NIH, Bethesda, MD, USA). The intensity of the signal was quantified using the Image J software in an area of 0.17 mm^2 located between the dentate gyrus and the CA1 region of the hippocampus, and expressed as the number of pixels/mm^2. The significance level (Student's t-test) was set at * $p < 0.05$, ** $p < 0.01$ and *** $p < 0.001$.

RNA purification

Total RNA from the posterior part of the neocortex and hippocampus of WT, *Epm2a*$^{-/-}$ and *Epm2b*$^{-/-}$ animals aged 16 days, 3 months and 12 months (n=7 per group) was isolated with the Rneasy Lipid Tissue Mini Kit (Qiagen® GmbH, Hilden, Germany) following the manufacturer's protocol. RNA concentration of each sample was measured using a NanoDrop™ Spectrophotometer (Thermo Fisher Scientific, Wilmington, DE, USA). RNA integrity number (RIN) was tested using the Agilent 2100 BioAnalyzer (Agilent Technologies, Palo Alto, CA, USA).

TaqMan qRT-PCR

cDNA was prepared using the High-Capacity cDNA Reverse Transcription kit (Applied Biosystems, Foster City, CA, USA) following the protocol provided by the supplier. Parallel reactions for each RNA sample were run in the absence of MultiScribe Reverse Transcriptase to assess the lack of contamination of genomic DNA. TaqMan qRT-PCR assays were performed in duplicate for each gene on cDNA samples in 384-well optical plates using an ABI Prism 7900 Sequence Detection system (Applied Biosystems, Life Technologies, Waltham, MA, USA). For each 10μL TaqMan reaction, 4.5μL cDNA was mixed with 0.5μL 20x TaqMan Gene Expression Assays and 5μL of 2× TaqMan Universal PCR Master Mix (Applied Biosystems). The identification numbers and names of TaqMan probes are shown in Table I. The mean values of the three house-keeping genes, hypoxanthine-guanine phosphoribosyltranferase (*Hprt*), alanyl-transfer RNA synthase (*Aars*) and X-prolyl aminopeptidase (aminopeptidaseP) 1 (*Xpnpep1*), were used as internal controls for normalization. The reactions were carried out using the following parameters: 50°C for 2min, 95°C for 10min, and 40 cycles of 95°C for 15sec and 60°C for 1min. Finally, all TaqMan PCR data were captured using the Sequence Detection Software (SDS version 2.2.2, Applied Biosystems). Samples were analyzed with the double-delta cycle threshold (ΔΔCT) method. Results were analyzed with two-way ANOVA followed by Tukey's post hoc or Student's t-test when required. The significance level was set at * $p < 0.05$, ** $p < 0.01$ and *** $p < 0.001$.

Western blotting

Mouse brain homogenates were lysed in RIPA buffer (50 mM Tris-HCl, pH 7.0; 150 mM NaCl, 1% Nonidet P-40; 0.5% Na-deoxycholate; 0.1% SDS) supplemented with protease and phosphatase inhibitors (Roche, Germany). After centrifugation at 14,000 g for 20 minutes at 4°C (Ultracentrifuge Beckman with 70Ti rotor), supernatants were quantified with BCA reagent (Pierce, Waltham, MA, USA). Protein samples were mixed with loading

sample buffer and heated at 95°C for 5 min. Twenty μg of proteins was separated by electrophoresis in SDS-PAGE gels and transferred to nitrocellulose membranes (200 mA per membrane, 80 minutes). Nonspecific binding was blocked by incubation in 5% non-fat milk in TBS containing 0.2% Tween for 1 hour at room temperature. The membranes were incubated at 4°C overnight with primary antibodies: anti-IL1β (diluted 1:1000, Abcam, Cambridge, United Kingdom), anti-IL6 (diluted 1:1000; Abcam, Cambridge, United Kingdom), anti-TNFα (diluted 1:1000, Abcam, Cambridge, United Kingdom) and anti-β-actin (diluted 1:30,000; Sigma-Aldrich, St. Louis, MO, USA). Membranes were washed with TBS-T and incubated for 1h at room temperature with the appropriate horseradish peroxidase conjugated secondary antibody (1:2,000; Dako, Glostrup, Denmark). Immune complexes were revealed by incubating the membranes with chemiluminescence reagent (electrochemiluminescence; Amersham, GE Healthcare, Buckinghamshire, United Kingdom). Densitometries were carried out with Totallab software (TL100 v.2006b), and values were normalized using β-actin levels. Normalized values were expressed as fold change from values obtained in WT aged 16 days samples.

Results

Lafora inclusions in the telencephalon in *Epm2a*$^{-/-}$ and *Epm2b*$^{-/-}$ mice

A few PAS-positive round or elongated inclusions in the neuropil and more rarely in the neuronal cytoplasm were first seen in transgenic mice aged 3 months. The number and size of the inclusions was higher in *Epm2a*$^{-/-}$ and *Epm2b*$^{-/-}$ mice aged 12 months as detailed elsewhere [16, 17]. Examples of these deposits are shown in Fig 1.

Astrocyte and microglial responses in *Epm2a*$^{-/-}$ and *Epm2b*$^{-/-}$ mice

We analyzed by immunohistochemistry the levels of GFAP (glial fibrillary acidic protein; a marker of reactive astrocytes) and Iba1 (ionized calcium-binding adapter molecule 1; a marker of reactive microglia) in selected brain areas from wild type (WT), *Epm2a*$^{-/-}$ and *Epm2b*$^{-/-}$ mice of 16 days, 3 months and 12 months of age. We observed that GFAP-immunoreactive astrocytes increased in number in the hippocampus (Fig. 2) and cerebral cortex (not shown) of *Epm2a*$^{-/-}$ and *Epm2b*$^{-/-}$ mice in comparison to WT littermates, at 3 and 12 months of age. No significant differences were found between *Epm2a*$^{-/-}$ and *Epm2b*$^{-/-}$ mice. Iba1-immunoreactive microglia also increased in number in *Epm2a*$^{-/-}$ and *Epm2b*$^{-/-}$ mice when compared to WT littermates at the age of 3 and 12 months (Fig. 3). In addition, we found that the number of reactive microglial cells was greater in *Epm2b*$^{-/-}$ when compared to *Epm2a*$^{-/-}$ mice (Fig. 3).

Gene expression of cytokines and mediators of the inflammatory response with aging in WT, *Epm2a*$^{-/-}$ and *Epm2b*$^{-/-}$ mice

Since reactive astrocytes and microglia are mediators of the innate inflammatory response, we assessed the age-dependent expression of a panel of cytokines and mediators of the inflammatory response in wild type, *Epm2a*$^{-/-}$ and *Epm2b*$^{-/-}$ mice. First, we analyzed the regular age-dependent changes in the expression of these genes in wild type mice: we found that *C3ar1*, *C4b*, *Csf3r*, *Ccl6*, *CxCl10*, *Il6*, *Il6st*, *Tnfrsf1a*, *Il10ra* and *Il10rb* mRNA expression levels significantly increased and *C1ql1* levels significantly decreased in WT

mice of 3 months of age when compared with WT mice aged 16 days. The differences in the expression levels of these genes further increased in WT mice aged 12 months when compared with mice aged 16 days; in addition, *Ccl3*, *Ccl4*, *Tlr4* and *Tnfα* mRNA expression was higher in WT mice aged 12 months when compared with mice aged 16 days. However, *Tgf-β1* decreased with age. Increased expression with age was supported to a greater extent by the fact that *C4b*, *Ccl3*, *Ccl4*, *Ccl6*, CxCl10, *Il6*, and *Tnfα* were significantly increased in WT mice aged 12 months when compared with WT mice 3 months old (Table II).

In the case of *Epm2a*$^{-/-}$ mice, *C3ar1*, *Csf3r*, *Ccl4, Il1b, Il6st*, *Il10ra*, and *Il10rb* mRNAs were increased and *C1ql1* mRNA was decreased in mice aged 3 months when compared with mice aged 16 days. Moreover, *C3ar1*, *C4b*, *Csf1r*, *Csf3r*, *Tlr4*, *Ccl4*, *Ccl6*, *CxCl10*, *Il1b*, *Il6*, *Tnfα*, *Il10ra* and *Il10rb* mRNAs were significantly increased in *Epm2a*$^{-/-}$ aged 12 months when compared with *Epm2a*$^{-/-}$ aged 16 days. *C1ql1* mRNA also significantly decreased in *Epm2a*$^{-/-}$ mice aged 12 months. Finally, nine genes, *C3ar1*, *C4b*, *Csfr1*, *Csf3r*, *Ccl6*, *CxCl10*, *Il1b*, *Il6* and *Tnfα*, were significantly up-regulated in *Epm2a*$^{-/-}$ aged 12 months when compared with *Epm2a*$^{-/-}$ aged 3 months (Table II).

Regarding modifications in gene expression with aging in *Epm2b*$^{-/-}$ mice, *C3ar1*, *Ccl6*, *Il6*, *Il6st*, and *Il10rb* mRNA expression was increased and C1ql1 mRNA levels were downregulated in mice aged 3 months when compared with 16-day-old mice. *C3ar1*, C4b, Csf3r, *Tlr4*, *Ccl3*, *Ccl4*, *Ccl6*, *CxCl10*, *Il1b, Il6, Il6st*, *Tnfα, Tnfrsf1a, Il10*, *Il10ra* and *Il10rb* were significantly increased in *Epm2b*$^{-/-}$ mice aged 12 months when compared with *Epm2b*$^{-/-}$ mice aged 16 days. In contrast, a significant reduction in *C1ql1* mRNA levels was observed in *Epm2b*$^{-/-}$ mice aged 12 months when compared with younger animals. Differences with age were greater in *Epm2b*$^{-/-}$ when compared with *Epm2a*$^{-/-}$ mice, as thirteen genes instead of nine genes were significantly up-regulated in *Epm2b*$^{-/-}$ mice aged 12 months when compared with mice aged 3 months, including *C3ar1*, C4b, *Tlr4*, *Tlr7*, *Ccl3*, *Ccl4*, *Ccl6*, *CxCl10*, *Il1b*, Il6, *Tnfα*, *Il10ra* and *Il10rb* (Table II).

Differential gene expression of cytokines and mediators of the inflammatory response in *Epm2a*$^{-/-}$ and *Epm2b*$^{-/-}$ mice compared with WT mice

Then, we analyzed the differences in gene expression at the different ages between wild type, *Epm2a*$^{-/-}$ and *Epm2b*$^{-/-}$ mice. Few differences were seen in *Epm2a*$^{-/-}$ (laforin knock-out) and *Epm2b*$^{-/-}$ (malin knock-out) mice aged 16 days when compared with age-matched WT littermates; we found a small increase in the expression of *Il6* and *Tnfα* in *Epm2a*$^{-/-}$ mice and a small increase in the expression of *C1qtnf7*, *Csf3r* and *Il6* in *Epm2b*$^{-/-}$ mice at this age (Table II). At 3 months of age we found an increase in the expression of *Ccl4*, *CxCl10* and *Il6st* in *Epm2a*$^{-/-}$ mice, and of *CxCCl10* and *Tnfα* in *Epm2b*$^{-/-}$ mice (Table II). In contrast, a significant reduction of *Ccl4* and *Il10ra* occurred in *Epm2b*$^{-/-}$ when compared with *Epm2a*$^{-/-}$ mice at this age. However, a dramatic gene up-regulation was found in *Epm2b*$^{-/-}$ mice at the age of 12 months when compared with the limited change in *Epm2a*$^{-/-}$ mice at a similar age. Whereas only *C3ar1, Csf3r* and *CxCl10* mRNA expression was increased in *Epm2a*$^{-/-}$ in comparison to WT, the expression of *C3ar1, C4b, Ccl4, Ccl6, CxCl10, Il1b, Il6, Tnfα* and *Il10ra* was up-regulated in *Epm2b*$^{-/-}$ aged 12 months when compared with age-matched WT (Table II). All these results are compatible with the

presence of inflammation in the brain of LD mice at 3 months of age becoming aggravated as the mice aged, with the phenotype more severe in the case of *Epm2b*$^{-/-}$ mice. In fact, *C3ar1, Ccl4, Ccl6, CxCl10, Il1b, tnfα* and *Il10ra* mRNA expression was significantly up-regulated in *Emp2b*$^{-/-}$ mice aged 12 months when compared with *Epm2a*$^{-/-}$ mice of the same age (Table II).

Protein expression of selected cytokines and mediators

In order to confirm the inflammatory process present in the brain of *Epm2a*$^{-/-}$ and *Epm2b*$^{-/-}$ mice, IL1-β, IL6 and TNFα protein levels were analyzed by western blotting in brain extracts from wild type, *Epm2a*$^{-/-}$ and *Epm2b*$^{-/-}$ mice at the ages of 16 days, 3 months and 12 months. As shown in Fig. 4, at 16 days of age *Epm2b*$^{-/-}$ mice showed an increase in the levels of IL1-β and IL6 in comparison to WT mice. No differences were observed in the case of *Epm2a*$^{-/-}$ mice. At 3 months of age, we found in *Epm2b*$^{-/-}$ mice a tendency to higher levels of IL1-β and IL6 and a significant increase in the levels of TNFα in comparison to WT of the same age. However, *Epm2a*$^{-/-}$ mice showed similar protein levels of IL1-β and IL6 and reduced levels of TNF-α at this age in comparison to WT. At 12 months of age, *Epm2b*$^{-/-}$ mice showed higher levels of IL1-β and IL6 but similar levels of TNFα in comparison to WT of the same age. In contrast, *Epm2a*$^{-/-}$ mice showed levels of IL1-β, IL6 and TNFα similar to WT. These data confirm that *Epm2b*$^{-/-}$ mice present a more severe inflammatory pattern than *Epm2a*$^{-/-}$ mice.

In addition, we analyzed the levels of cyclooxigenase 2 (Cox2), a target gene of inflammatory mediators. An immunohistochemical analysis of the hippocampus of WT, *Epm2a*$^{-/-}$ and *Epm2b*$^{-/-}$ mice of different ages showed an increase in the levels of Cox2 in the case of *Epm2a*$^{-/-}$ and *Epm2b*$^{-/-}$ mice at 3 months of age, which dramatically increased at 12 months of age (Fig. 5), with the staining at this age more intense in the case of *Epm2b*$^{-/-}$ in comparison to *Epm2a*$^{-/-}$ mice.

Discussion

Laforin knock-out (*Epm2a*$^{-/-}$) and malin knock-out (*Epm2b*$^{-/-}$) mice used in the present study [17, 31] start to develop LBs in cerebral cortex, hippocampus, basal ganglia, thalamus, cerebellum, cerebellar nuclei and brain stem at about the first month of age, and this increases in number and size with disease progression. LBs are very abundant in these regions at advanced stages of the disease [17, 31, 32]. Deposits are also found in the choroid plexus but the olfactory bulb is largely spared. Although both mouse lines have clinical symptoms similar to those seen in human LD, *Epm2b*$^{-/-}$ mice show some differences in comparison to *Epm2a*$^{-/-}$ mice such as reduced accumulated motor surface, rearing and stereotyped activity, as well as lower episodic memory deficits and non-spatial memory skills. In addition, although both mouse lines have tonic-clonic seizures, these occur in parallel with spike-wave, poly-spikes and poly-spike-wave complexes in *Epm2a*$^{-/-}$ mice but there are no EEG correlates in *Epm2b*$^{-/-}$ mice [32]. All these data suggest that the phenotype observed in *Epm2b*$^{-/-}$ mice is more severe than that presented in *Epm2a*$^{-/-}$ mice.

In this study, we investigated whether neuroinflammation is a novel hallmark in Lafora disease. With this aim, we analyzed how the expression of a panel of cytokines and

mediators of the inflammatory response changes with age in WT, *Epm2a*$^{-/-}$ and *Epm2b*$^{-/-}$ mice. It is known that marked modification of the profile of gene expression of cytokines and molecules linked with the inflammatory response occurs in the cerebral cortex and other brain regions of mice with age. This happens in normal aging and also in transgenic mice including APP/PS1, *P301S-MAPT* and S49P-Syracuse human neuroserpin (S49P-Syracuse), and in CJD-induced prionopathy in murine PrP-null mice expressing human PrP, which are models of human β-amyloidopathy reminiscent of Alzheimer disease, familial frontotemporal degeneration-tauopathy (FTLD-tau), neuroserpinopathy and Creutzfeldt-Jakob disease, respectively [33–36]. This pattern is repeated in our study as *C3ar1*, *C4b*, *Csf3r*, *Tlr4*, *Ccl4, Ccl6*, *CxCl10*, *Il1b, Il6*, *Tnfα, Il10ra* and *Il10rb* mRNA expression levels increase and *C1ql1* levels significantly decrease in WT, *Epm2a*$^{-/-}$ and *Epm2b*$^{-/-}$ mice aged 12 months when compared with mice aged 16 days. At the same time, *Ccl3, Il6st and Tgfb1* are increased only in WT and *Epm2a*$^{-/-}$ mice whereas *Tnfrsf1a* and *Il10* increased only in *Epm2b*$^{-/-}$ mice. These findings support the idea that gene expression of cytokines and mediators of the inflammatory response is modulated with age, albeit with genotypic variations.

Focusing on pathologic states, inflammatory responses are increased in *Epm2a*$^{-/-}$ and *Epm2b*$^{-/-}$ mice when compared with WT littermates. *C3ar1, Csf3r* and *CxCl10* are significantly increased in *Epm2a*$^{-/-}$ mice aged 12 months when compared with age-matched controls. Curiously, inflammatory responses are greater in *Epm2b*$^{-/-}$ mice when compared with *Epm2a*$^{-/-}$ mice, as *C3ar1*, *C4b, Ccl4*, *Ccl6, CxCl10*, *Il1b*, *Il6*, *Tnfα* and *Il10ra* mRNAs are significantly up-regulated in *Epm2b*$^{-/-}$ aged 12 months. In general terms, IL1-β, IL6 and TNFα protein levels are in accordance with the corresponding mRNA expression levels, with the *Epm2b*$^{-/-}$ genotype the most dramatically affected. However, a discrepancy exists between *Tnfα* mRNA and TNFα protein levels at the age of 3 months in *Epm2a*$^{-/-}$. It can be suggested that unexpected reduced TNFα protein expression is related to epigenetic regulation. However there is no available information about non-coding RNAs in LD and related transgenic models. An explanation of this punctual finding at the age of 3 months in *Epm2a*$^{-/-}$ is not known. In agreement with increased expression of cytokines and mediators of the immune response in both LD mouse models, we found increased levels of Cox2, a protein with pro-inflammatory properties, in both *Epm2a*$^{-/-}$ and *Epm2b*$^{-/-}$ mice, although we observed higher protein levels in *Epm2b*$^{-/-}$ mice as the animals aged.

We also present data indicating that the number of GFAP-immunoreactive astrocytes increases in *Epm2a*$^{-/-}$ and *Epm2b*$^{-/-}$ mice when compared with WT littermates, although this increase is similar in *Epm2a*$^{-/-}$ and in *Epm2b*$^{-/-}$ mice. Therefore, the extent of dysregulated gene expression of cytokines and mediators of the inflammatory response, which is higher in *Epm2b*$^{-/-}$ mice, cannot be explained by a differing number of reactive astrocytes. However, we also present evidence of an increase in Iba-1-immunoreactive cells (microglia) in *Epm2a*$^{-/-}$ and *Epm2b*$^{-/-}$ mice, which is greater in *Epm2b*$^{-/-}$ mice in comparison to *Epm2a*$^{-/-}$ mice. This phenotype correlates with the increased gene expression of cytokines and mediators of the inflammatory response present in *Epm2b*$^{-/-}$ mice, suggesting involvement of reactive microglia in the severity of the inflammatory phenotype of *Emp2b*$^{-/-}$ mice.

Therefore, and in agreement with previous data [32], the phenotype in *Epm2b*$^{-/-}$ mice is more severe than in the *Epm2a*$^{-/-}$ *mice.* The causes of the more severe phenotype in *Epm2b*$^{-/-}$ are not known but our present results clearly show a close relationship between stronger microglia-dependent inflammatory responses and the already described impaired motor function, memory and learning, together with the unpredictable seizures present in these mice. Microglia may have very disparate functions depending on the setting and stimulus [37], but chronic inflammation, involving chemokines, pro-inflammatory cytokines, anti-inflammatory cytokines and members of the complement system, is usually associated with nerve cell damage in human neurodegenerative diseases with abnormal protein aggregates and in related animals models. The observations presented in this study are particularly relevant since increased microglia and marked increase in mRNA and protein expression of cytokines and mediators of the inflammatory response are described for the first time in LD, a paradigm of polyglucosan disease. Insoluble phosphorylated polyglucosans, endoplasmic reticulum stress, oxidative stress, altered autophagy and ubiquitin-proteasome activity may all contribute to the inflammatory response. Since inflammatory responses appear at relatively early stages of LD, the administration of anti-inflammatory agents may be considered a possible treatment in order to delay brain damage.

Acknowledgments

This study was funded by the Ministerio de Ciencia e Innovación, Instituto de Salud Carlos III – Fondos FEDER, a way to build Europe FIS grants PI14/00757 and PI14/00328 to IF, and grants from the Spanish Ministry of Economy and Competiveness SAF2014-54604-C3-1-R and from the Generalitat Valenciana (PrometeoII/2014/029) to PS. We thank T. Yohannan for editorial assistance.

References

1. Delgado-Escueta AV. Advances in lafora progressive myoclonus epilepsy. Curr Neurol Neurosci rep. 2007; 7:428–433. [PubMed: 17764634]
2. Monaghan TS, Delanty N. Lafora disease: epidemiology, pathophysiology and management. CNS drugs. 2010; 24:549–561. [PubMed: 20527995]
3. Lohi H, Ianzano L, Zhao XC, Chan EM, Turnbull J, Scherer SW, Ackerley CA, Minassian BA. Novel glycogen synthase kinase 3 and ubiquitination pathways in progressive myoclonus epilepsy. Hum Mol Genet. 2005; 14:2727–2736. [PubMed: 16115820]
4. Rubio-Villena C, Garcia-Gimeno MA, Sanz P. Glycogenic activity of R6, a protein phosphatase 1 regulatory subunit, is modulated by the laforin-malin complex. Int J Biochem Cell Biol. 2013; 45:1479–1488. [PubMed: 23624058]
5. Worby CA, Gentry MS, Dixon JE. Malin decreases glycogen accumulation by promoting the degradation of protein targeting to glycogen (PTG). J Biol Chem. 2008; 283:4069–4076. [PubMed: 18070875]
6. Solaz-Fuster MC, Gimeno-Alcaniz JV, Ros S, Fernandez-Sanchez ME, Garcia-Fojeda B, Criado Garcia O, Vilchez D, Dominguez J, Garcia-Rocha M, Sanchez-Piris M, Aguado C, Knecht E, Serratosa J, Guinovart JJ, Sanz P, Rodriguez de Cordoba S. Regulation of glycogen synthesis by the laforin-malin complex is modulated by the AMP-activated protein kinase pathway. Hum Mol Genet. 2008; 17:667–678. [PubMed: 18029386]
7. Wang J, Stuckey JA, Wishart MJ, Dixon JE. A unique carbohydrate binding domain targets the Lafora disease phosphatase to glycogen. J Biol Chem. 2002; 277:2377–2380. [PubMed: 11739371]
8. Worby CA, Gentry MS, Dixon JE. Laforin, a dual specificity phosphatase that dephosphorylates complex carbohydrates. J Biol Chem. 2006; 281:30412–30418. [PubMed: 16901901]
9. Tagliabracci VS, Turnbull J, Wang W, Girard JM, Zhao X, Skurat AV, Delgado-Escueta AV, Minassian BA, Depaoli-Roach AA, Roach PJ. Laforin is a glycogen phosphatase, deficiency of

which leads to elevated phosphorylation of glycogen in vivo. Proc Natl Acad Sci U S A. 2007; 104:19262–19266. [PubMed: 18040046]

10. Garyali P, Siwach P, Singh PK, Puri R, Mittal S, Sengupta S, Parihar R, Ganesh S. The malin-laforin complex suppresses the cellular toxicity of misfolded proteins by promoting their degradation through the ubiquitin-proteasome system. Hum Mol Genet. 2009; 18:688–700. [PubMed: 19036738]
11. Liu Y, Wang Y, Wu C, Liu Y, Zheng P. Deletions and missense mutations of EPM2A exacerbate unfolded protein response and apoptosis of neuronal cells induced by endoplasm reticulum stress. Hum Mol Genet. 2009; 18:2622–2631. [PubMed: 19403557]
12. Vernia S, Rubio T, Heredia M, Rodriguez de Cordoba S, Sanz P. Increased endoplasmic reticulum stress and decreased proteasomal function in Lafora disease models lacking the phosphatase laforin. PloS one. 2009; 4:e5907. [PubMed: 19529779]
13. Zeng L, Wang Y, Baba O, Zheng P, Liu Y. Laforin is required for the functional activation of malin in endoplasmic reticulum stress resistance in neuronal cells. The FEBS journal. 2012; 279(14): 2467–2478. [PubMed: 22578008]
14. Rao SN, Maity R, Sharma J, Dey P, Shankar SK, Satishchandra P, Jana NR. Sequestration of chaperones and proteasome into Lafora bodies and proteasomal dysfunction induced by Lafora disease-associated mutations of malin. Hum Mol Genet 2010a. 2010; 19:4726–4734.
15. Rao SN, Sharma J, Maity R, Jana NR. Co-chaperone CHIP stabilizes aggregate-prone malin, a ubiquitin ligase mutated in Lafora disease. J Biol Chem. 2010; 285:1404–1413. [PubMed: 19892702]
16. Aguado C, Sarkar S, Korolchuk VI, Criado O, Vernia S, Boya P, Sanz P, de Cordoba SR, Knecht E, Rubinsztein DC. Laforin, the most common protein mutated in Lafora disease, regulates autophagy. Hum Mol Genet. 2010; 19:2867–2876. [PubMed: 20453062]
17. Criado O, Aguado C, Gayarre J, Duran-Trio L, Garcia-Cabrero AM, Vernia S, San Millan B, Heredia M, Roma-Mateo C, Mouron S, Juana-Lopez L, Dominguez M, Navarro C, Serratosa JM, Sanchez M, Sanz P, Bovolenta P, Knecht E, Rodriguez de Cordoba S. Lafora bodies and neurological defects in malin-deficient mice correlate with impaired autophagy. Hum Mol Genet. 2012; 21:1521–1533. [PubMed: 22186026]
18. Garcia-Gimenez JL, Seco-Cervera M, Aguado C, Roma-Mateo C, Dasi F, Priego S, Markovic J, Knecht E, Sanz P, Pallardo FV. Lafora disease fibroblasts exemplify the molecular interdependence between thioredoxin 1 and the proteasome in mammalian cells. Free Radic Biol Med. 2013; 65:347–359. [PubMed: 23850970]
19. Roma-Mateo C, Aguado C, Garcia-Gimenez JL, Ibanez-Cabellos JS, Seco-Cervera M, Pallardo FV, Knecht E, Sanz P. Increased oxidative stress and impaired antioxidant response in Lafora disease. Mol Neurobiol. 2015; 51:932–946. [PubMed: 24838580]
20. Roma-Mateo C, Aguado C, Luis Garcia-Gimenez J, Knecht E, Sanz P, Pallardo FV. Oxidative stress, a new hallmark in the pathophysiology of Lafora progressive myoclonus epilepsy. Free Radic Biol Med. 2015 doi:S0891-5849(15)00043-X [pii].
21. Kiffin R, Bandyopadhyay U, Cuervo AM. Oxidative stress and autophagy. Antioxid Redox Signal 2006. 2006; 8:152–162.
22. Lee J, Giordano S, Zhang J. Autophagy, mitochondria and oxidative stress: cross-talk and redox signalling. Biochem J. 2012; 441:523–540. [PubMed: 22187934]
23. Dutta D, Xu J, Kim JS, Dunn WA Jr, Leeuwenburgh C. Upregulated autophagy protects cardiomyocytes from oxidative stress-induced toxicity. Autophagy 2013. 2013; 9:328–344.
24. Navarro-Yepes J, Burns M, Anandhan A, Khalimonchuk O, Del Razo LM, Quintanilla-Vega B, Pappa A, Panayiotidis MI, Franco R. Oxidative stress, redox signaling, and autophagy: cell death versus survival. Antioxid Redox Signal. 2014; 21:66–85. [PubMed: 24483238]
25. Duran J, Gruart A, Garcia-Rocha M, Delgado-Garcia JM, Guinovart JJ. Glycogen accumulation underlies neurodegeneration and autophagy impairment in Lafora disease. Hum Mol Genet. 2014; 23:3147–3156. [PubMed: 24452334]
26. Berthier A, Paya M, Garcia-Cabrero AM, Ballester MI, Heredia M, Serratosa JM, Sanchez MP, Sanz P. Pharmacological interventions to ameliorate neuropathological symptoms in a mouse model of Lafora disease. Mol Neurobiol. 2015; doi: 10.1007/s12035-015-9091-8

27. McGeer EG, Klegeris A, McGeer PL. Inflammation, the complement system and the diseases of aging. Neurobiol Aging. 2005; 26(Suppl 1):94–97. [PubMed: 16198446]
28. Graeber MB, Streit WJ. Microglia: biology and pathology. Acta Neuropathol 2010. 2010; 119:89–105.
29. Heneka MT, Kummer MP, Latz E. Innate immune activation in neurodegenerative disease. Nat Rev Immunol. 2014; 14:463–477. [PubMed: 24962261]
30. López González I, Garcia-Esparcia P, Llorens F, Ferrer I. Genetic and transcriptomic profiles of inflammation in neurodegenerative diseases: Alzheimer, Parkinson, Creutzfeldt-Jakob and tauopathies. Int J Mol Sci. 2016 (Epub ahead of print).
31. Ganesh S, Delgado-Escueta AV, Sakamoto T, Avila MR, Machado-Salas J, Hoshii Y, Akagi T, Gomi H, Suzuki T, Amano K, Agarwala KL, Hasegawa Y, Bai DS, Ishihara T, Hashikawa T, Itohara S, Cornford EM, Niki H, Yamakawa K. Targeted disruption of the Epm2a gene causes formation of Lafora inclusion bodies, neurodegeneration, ataxia, myoclonus epilepsy and impaired behavioral response in mice. Hum Mol Genet. 2002; 11:1251–1262. [PubMed: 12019206]
32. García-Cabrero AM, Marinas A, Guerrero R, de Córdoba SR, Serratosa JM, Sanchez MP. Laforin and malin deletions in mice produce similar neurologic impairments. J Neuropathol Exp Neurol. 2012; 71:413–421. [PubMed: 22487859]
33. Llorens F, López-González I, Thüne K, Carmona M, Zafar S, Andréoletti O, Zerr I, Ferrer I. Subtype and regional-specific neuroinflammation in sporadic Creutzfeldt-Jakob disease. Front Aging Neurosci. 2014; 6:198. [PubMed: 25136317]
34. López-González I, Aso E, Carmona M, Armand-Ugon M, Blanco R, Naudí A, Cabré R, Portero-Otin M, Pamplona R, Ferrer. Neuroinflammatory gene regulation, mitochondrial function, oxidative stress, and brain lipid modifications with disease progression in tau P301S transgenic mice as a model of frontotemporal lobar degeneration-tau. J Neuropathol Exp Neurol. 2015; 74:975–999. [PubMed: 26360374]
35. López-González I, Schlüter A, Aso E, Garcia-Esparcia P, Ansoleaga B, LLorens F, Carmona M, Moreno J, Fuso A, Portero-Otin M, Pamplona R, Pujol A, Ferrer I. Neuroinflammatory signals in Alzheimer disease and APP/PS1 transgenic mice: correlations with plaques, tangles, and oligomeric species. J Neuropathol Exp Neurol. 2015; 74:319–344. [PubMed: 25756590]
36. López-González I, Pérez-Mediavilla A, Zamarbide M, Carmona M, Torrejón Escribano B, Glatzel M, Galliciotti G, Ferrer I. Limited unfolded protein response and inflammation in neuroserpinopathy. J Neuropathol Exp Neurol. 2016 (Epub ahead of print).
37. Svahn AJ, Becker TS, Graeber MB. Emergent properties of microglia. Brain Pathol. 2014; 24:665–670. [PubMed: 25345896]

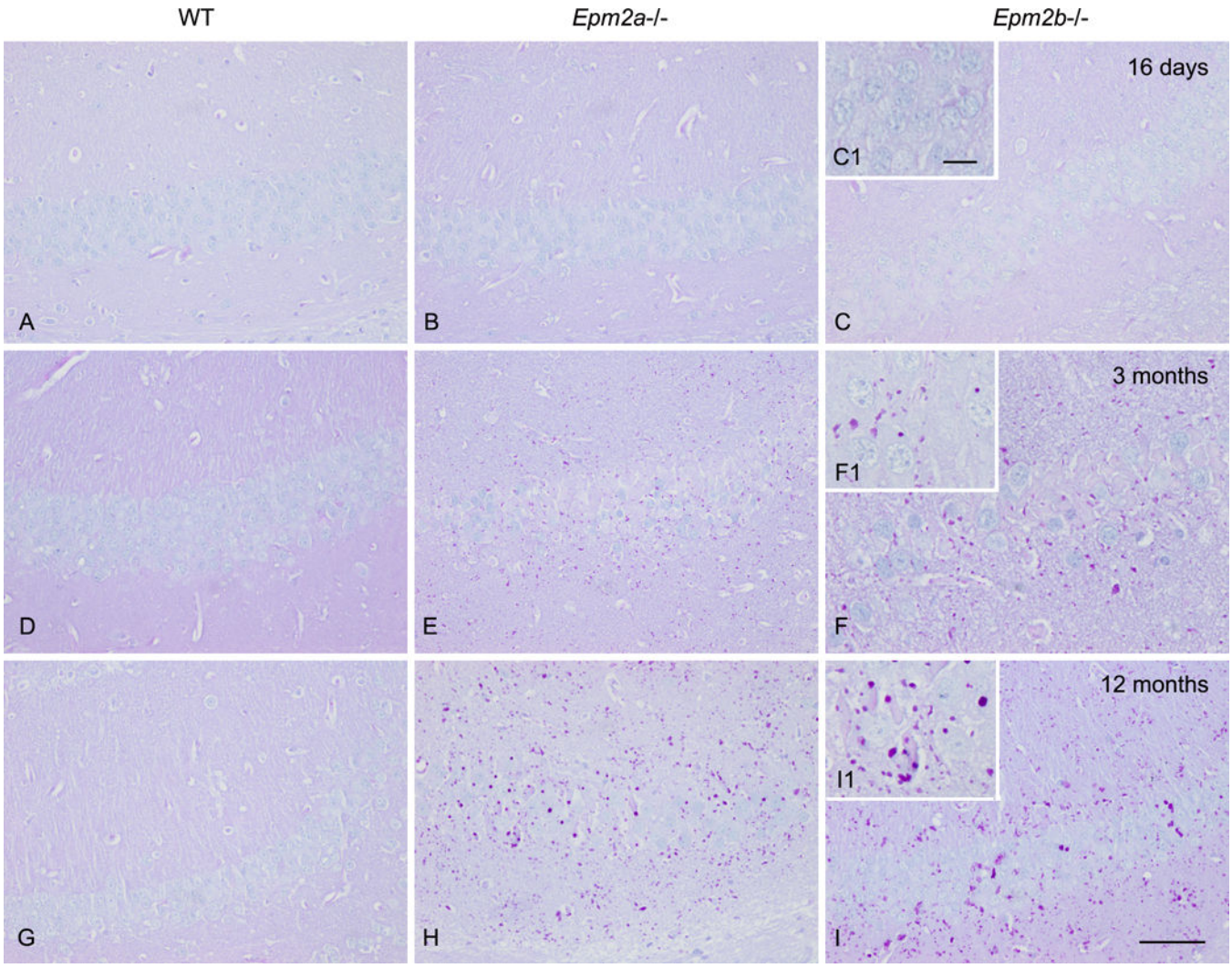

Figure 1.

Periodic acid-Schiff (PAS) staining of representative sections of the hippocampus of wild type (WT), *Epm2a*$^{-/-}$ (laforin knock-out) and *Epm2b*$^{-/-}$ (malin knock-out) mice aged 16 days, 3 months and 12 months. A-I: scale bar in I = 150 μm; C1, F1, I1, scale bar in C1 = 15 μm. A few PAS-positive inclusions are seen in *Epm2a*$^{-/-}$ and *Epm2b*$^{-/-}$ at the age of three months. The number and size of inclusions augments at the age of 12 months.

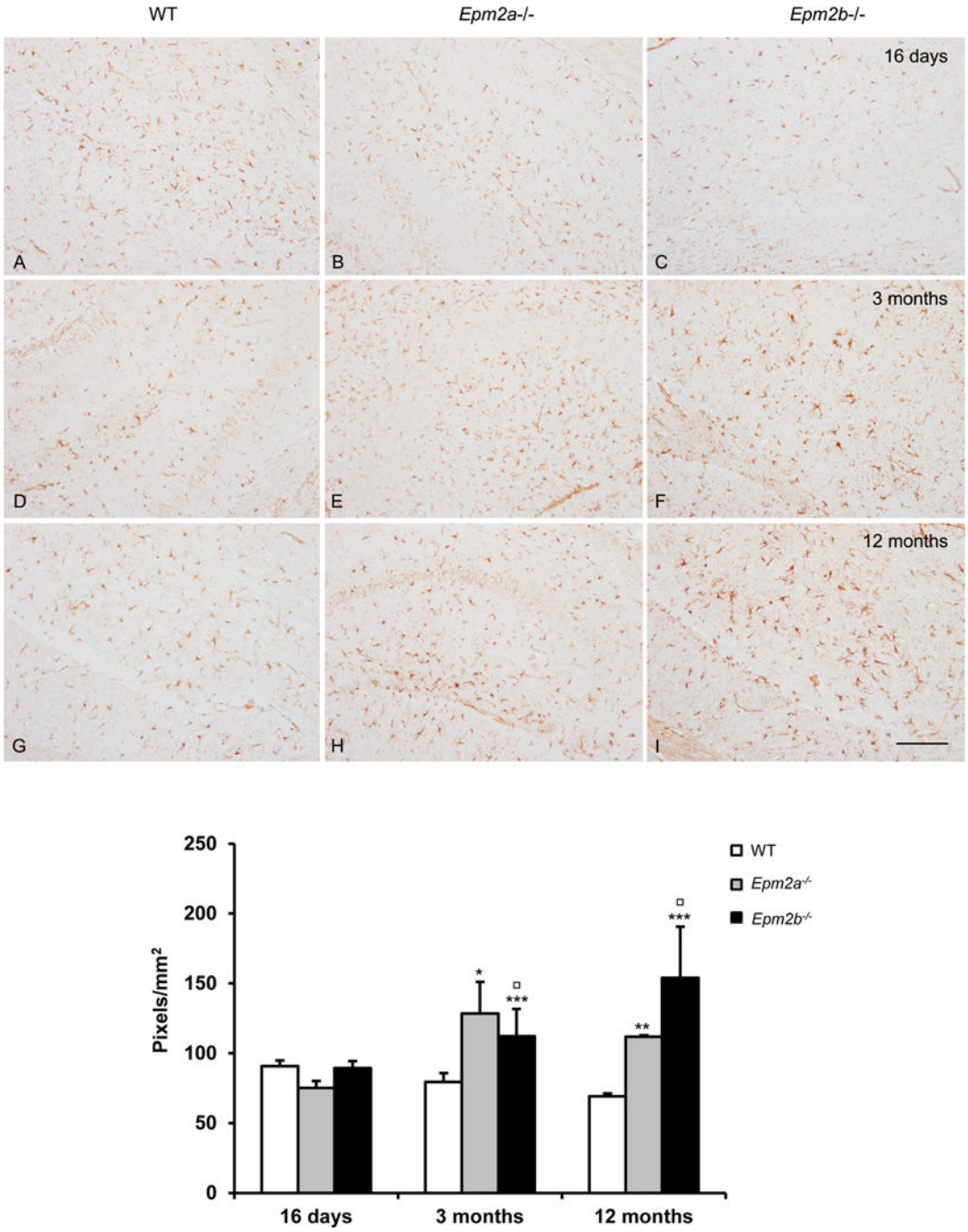

Figure 2.

Glial fibrillary acidic protein (GFAP) immunohistochemistry of the hippocampus of wild type (WT), *Epm2a*$^{-/-}$ (laforin knock-out) and *Epm2b*$^{-/-}$ (malin knock-out) mice aged 16 days, 3 months and 12 months. Paraffin sections slightly counterstained with hematoxylin. A-I, scale bar in I = 150 μm. The intensity of the signal was expressed as number of pixels/mm^2. Data are the mean values from at least three independent mice; vertical bars indicate standard deviation. Marked increase in the number of astrocytes is observed in the CA1 region of the hippocampus in *Epm2a*$^{-/-}$ and *Epm2b*$^{-/-}$ mice when compared with WT

at the age of 3 months and 12 months. Significant differences with respect to the corresponding WT are evaluated as * $p<0.05$, ** $p<0.01$, *** $p<0.001$ compared with age-matched WT (Student's t-test). No significant differences were observed between *Epm2a*$^{-/-}$ and *Epm2b*$^{-/-}$ mice in any age group.

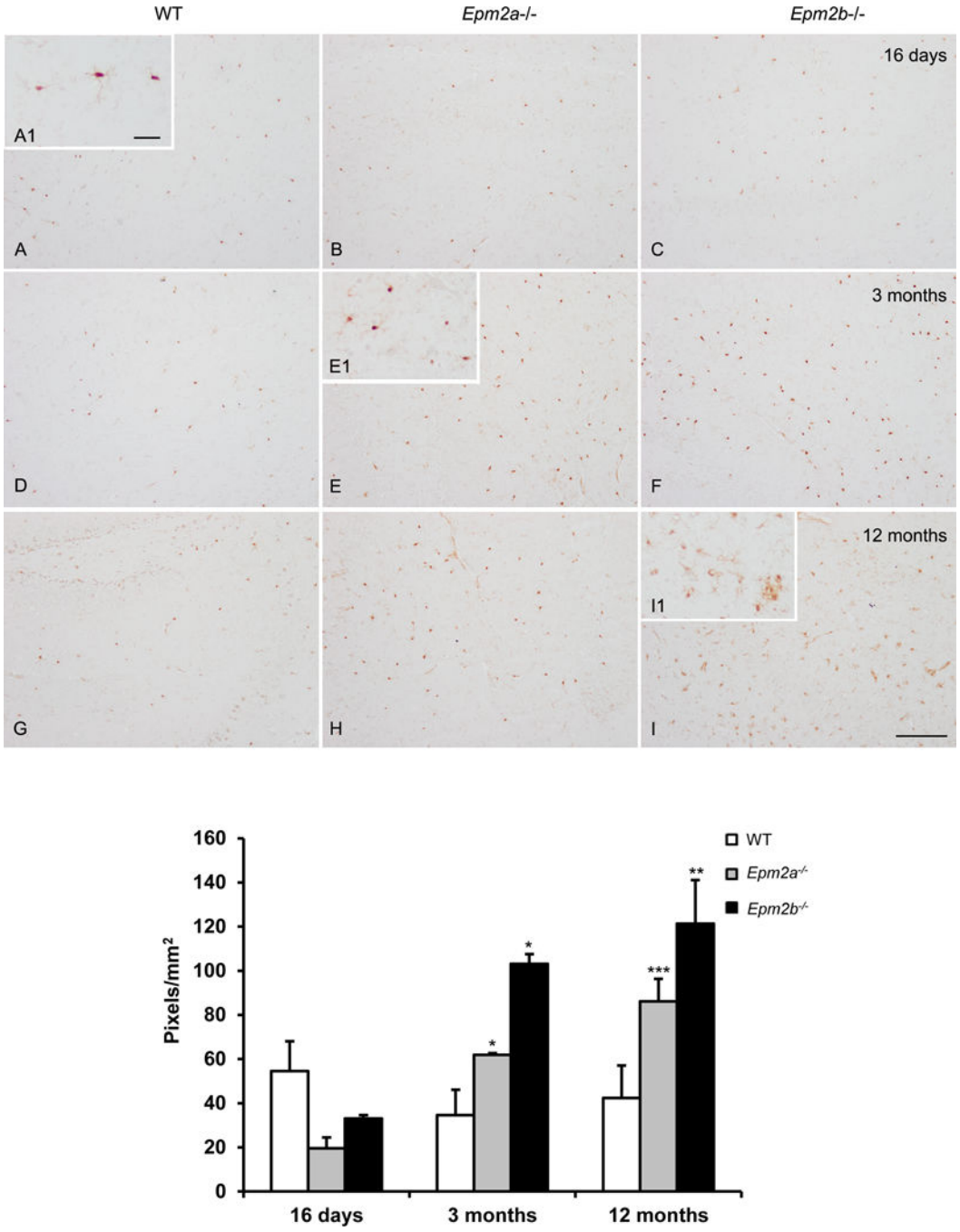

Figure 3.

Iba1 immunohistochemistry of the hippocampus of wild type (WT), *Epm2a*$^{-/-}$ (laforin knock-out) and *Epm2b*$^{-/-}$ (malin knock-out) mice aged 16 days, 3 months and 12 months. Paraffin sections slightly stained with hematoxylin. A-I, scale bar in I = 170 μm. A1, E1 and I1, scale bar in A1 = 15 μm. The intensity of the signal was expressed as the number of pixels/mm^2. Data are the mean values from at least three independent mice; vertical bars indicate standard deviation. Marked increase in the number of microglia is observed in the CA1 region of the hippocampus in *Epm2a*$^{-/-}$ and *Epm2b*$^{-/-}$ mice when compared with WT

at the age of 3 months and 12 months. Significant differences with respect to the corresponding WT are evaluated as * $p<0.05$, ** $p<0.01$, *** $p<0.001$ compared with age-matched WT. ¤ $p < 0.05$ compared with Epm2a−/− (Student's t-test).

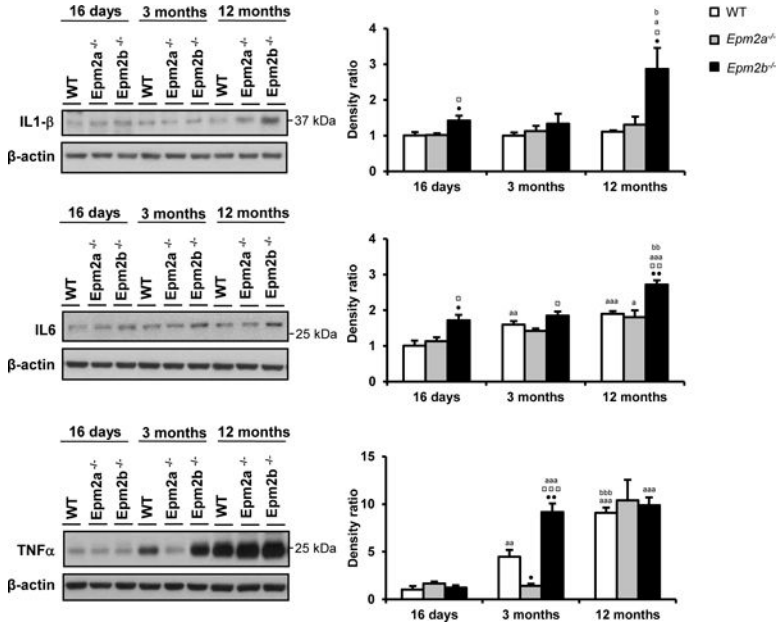

Figure 4.

Western blot of IL1-β, IL6 and TNF-α in wild-type (WT), *Epm2a*$^{-/-}$ (laforin knock-out) and *Epm2b*$^{-/-}$ (malin knock-out) mice aged 16 days, 3 months and 12 months. Data show an increase in IL1-β and IL6 protein levels in *Epm2b*$^{-/-}$ aged 16 days and 12 months when compared with age-matched WT. A significant reduction in TNF-α protein levels occurred in *Epm2a*$^{-/-}$ and an increase in *Epm2b*$^{-/-}$ aged 3 months when compared to WT. β-actin is used as a control of protein loading. Data are presented as the mean ± SEM. * $p < 0.05$, ** $p < 0.01$ and *** $p < 0.001$ compared with age-matched WT. ▫ $p < 0.05$, ▫▫ $p < 0.01$, ▫▫▫ $p < 0.001$ compared with *Epm2a*$^{-/-}$. ^{a} $p < 0.05$, ^{aa} $P < 0.01$, ^{aaa} $p < 0.001$ compared with animals aged 16 days. ^{b} $p < 0.05$, ^{bb} $p < 0.01$, ^{bbb} $p < 0.001$ compared with animals aged 3 months.

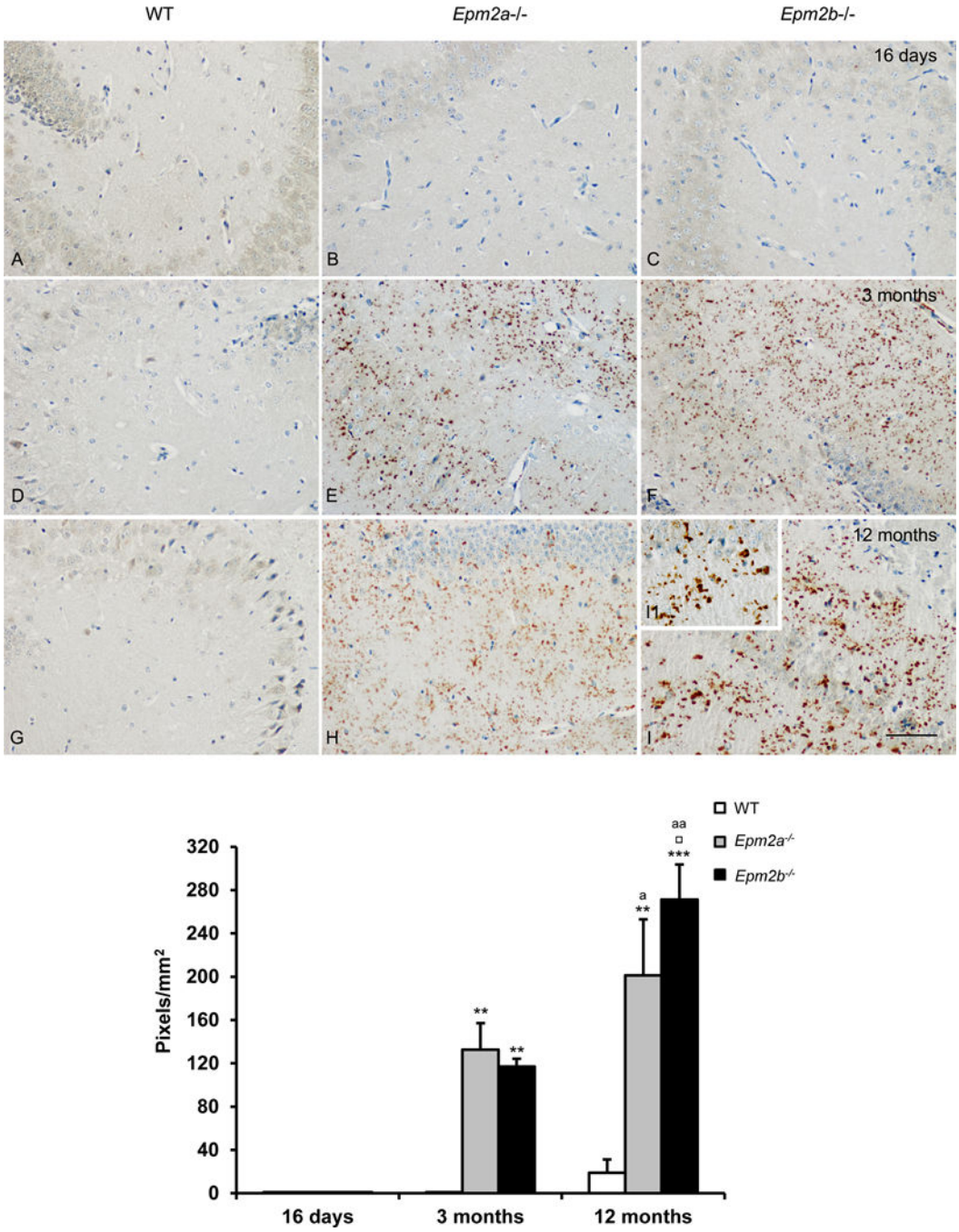

Figure 5.

Cox2 immunohistochemistry of the hippocampus of wild type (WT), *Epm2a*$^{-/-}$ (laforin knock-out) and *Epm2b*$^{-/-}$ (malin knock-out) mice aged 16 days, 3 months and 12 months. Paraffin sections slightly stained with hematoxylin. A-I, scale bar in I = 170 μm, I1, scale bar = 15 μm. The intensity of the signal was expressed as the number of pixels/mm^2. Data are the mean values from at least three independent mice; vertical bars indicate standard deviation. Marked increase in the levels of Cox2 is observed in the CA1 region of the hippocampus in *Epm2a*$^{-/-}$ and *Epm2b*$^{-/-}$ mice when compared with WT at the age of 3

months and 12 months. Significant differences with respect to the corresponding WT are evaluated as * p<0.05, ** p<0.01, *** p<0.001 compared with age-matched WT. ¤ p < 0.05 compared with Epm2a−/−; a p <0.05, aa P < 0.01 compared with animals aged 16 day (Student's t-test).

Table I

TaqMan probes used for the study of expression of cytokines and mediators of the immune response in mouse, including probes used for normalization (*Hprt*, *Aars* and *Xpnpep1*).

Symbol	Name of the gene	Reference
Hprt	Hypoxanthine-guanine phosphoribosyltranferase	Mm01545399_m1
Aars	Alanyl-tRNA synthase	Mm00507627_m1
Xpnpep1	X-prolyl aminopeptidase (aminopeptidase P) 1	Mm00460040_m1
C1ql1	Complement component 1, q subcomponent 1	Mm00657289_m1
C1qtnf7	C1q and tumor necrosis factor related protein 7	Mm00615171_m1
C3ar1	Complement component 3a receptor 1	Mm01184110_m1
C4b	Complement component 4b	Mm00437890_m1
Csf1r	Colony stimulating factor 1 receptor	Mm01266652_m1
Csf3r	Colony stimulating factor 1 receptor	Mm00432735_m1
Tlr4	Toll-like receptor 4	Mm00445273_m1
Tlr7	Toll-like receptor 7	Mm00446590_m1
Ccl3	Chemokine (C-C motif) ligand 3	Mm00441258_m1
Ccl4	Chemokine (C-C motif) ligand 4	Mm00443111_m1
Ccl6	Chemokine (C-C motif) ligand 6	Mm01302419_m1
CxCl10	Chemokine (C-X-C motif) ligand 10	Mm00445235_m1
Il1b	Interleukin 1β	Mm00434228_m1
Il6	Interleukin 6	Mm00446190_m1
Il6st	Interleukin 6 signal transducer	Mm00439665_m1
Tnfα	Tumor necrosis factor α	Mm99999068_m1
Tnfrsf1a	Tumor necrosis factor receptor superfamily member 1a	Mm01182929_m1
Il10	Interleukin 10	Mm00439614_m1
Il10ra	Interleukin 10 receptor α	Mm00434151_m1
Il10rb	Interleukin 10 receptor β	Mm00434157_m1
Tgb1	Transforming growth factor β1	Mm03024053_m1
Tgfb2	Transforming growth factor β2	Mm00436955_m1

Table II

mRNA expression of selected cytokine-related genes involved in the inflammatory response in wild-type (WT), *Epm2a*$^{-/-}$ (laforin knock-out) and *Epm2b*$^{-/-}$ (malin knock-out) mice aged 16 days, 3 months and 12 months. Data are represented as the mean ± SEM.

			16 days			3 months			12 months		
			WT	***Epm2a*$^{-/-}$**	***Epm2b*$^{-/-}$**	**WT**	***Epm2a*$^{-/-}$**	***Epm2b*$^{-/-}$**	**WT**	***Epm2a*$^{-/-}$**	***Epm2b*$^{-/-}$**
Activated pro-inflammatory cytokines	Complement system	*C1ql1*	1.00 ± 0.03	1.06 ± 0.02	1.01 ± 0.03	0.70 ± 0.03^{aaa}	0.75 ± 0.03^{aaa}	0.68 ± 0.03^{aaa}	0.66 ± 0.03^{aaa}	0.76 ± 0.03^{aaa}	0.78 ± 0.03^{aaa*}
		C1qtnf7	1.01 ± 0.05	1.27 ± 0.04	1.30 ± 0.12*	1.16 ± 0.06	1.20 ± 0.08	1.14 ± 0.07	1.09 ± 0.04	1.20 ± 0.05	1.28 ± 0.09
		C3ar1	1.01 ± 0.05	0.95 ± 0.03	0.95 ± 0.03	1.31 ± 0.03^{aaa}	1.22 ± 0.04^{a}	1.25 ± 0.05^{a}	1.37 ± 0.04^{aaa}	1.70 ± 0.09^{aaabbb*}	2.25 ± 0.14$^{aaabbb***¤¤}$
		C4b	1.00 ± 0.04	0.95 ± 0.04	0.99 ± 0.06	2.48 ± 0.22^{aaa}	2.88 ± 0.29	2.70 ± 0.18	5.03 ± 0.25^{aaabbb}	8.68 ± 1.23^{aaabbb}	14.17 ± 2.82^{aaabbb**}
	Colony stimulating factors receptors	*Csf1r*	1.01 ± 0.04	1.03 ± 0.07	1.05 ± 0.02	1.03 ± 0.03	1.07 ± 0.03	1.07 ± 0.05	1.07 ± 0.05	1.28 ± 0.06^{ab}	1.47 ± 0.30
		Csf3r	1.01 ± 0.06	0.97 ± 0.05	1.31 ± 0.10$^{*¤}$	1.76 ± 0.18^{aa}	1.81 ± 0.10^{aaa}	1.80 ± 0.12	1.70 ± 0.09^{aa}	2.46 ± 0.19^{aaabb*}	2.41 ± 0.34^{aa}
	TLRs	*Tlr4*	1.02 ± 0.08	0.95 ± 0.04	0.92 ± 0.03	0.96 ± 0.05	1.08 ± 0.05	1.01 ± 0.04	1.25 ± 0.06^{ab}	1.30 ± 0.10^{aa}	1.49 ± 0.18^{aabb}
		Tlr7	1.03 ± 0.11	0.89 ± 0.04	0.93 ± 0.10	0.76 ± 0.07	0.82 ± 0.04	0.81 ± 0.05	0.91 ± 0.05	1.03 ± 0.10	1.32 ± 0.20^{b}
Chemokines	CC subfamily	*Ccl3*	1.01 ± 0.07	1.29 ± 0.07	1.26 ± 0.21	1.00 ± 0.05	1.36 ± 0.22	1.01 ± 0.08	1.50 ± 0.14^{aabb}	1.82 ± 0.27	2.48 ± 0.40^{aabb}
		Ccl4	1.02 ± 0.09	1.14 ± 0.09	1.17 ± 0.07	1.53 ± 0.15	2.88 ± 0.20^{aaa***}	2.05 ± 0.18$^{¤}$	3.63 ± 0.34^{aaabbb}	3.77 ± 0.37^{aaa}	5.85 ± 0.65$^{aaabbb**¤}$
		Ccl6	1.01 ± 0.06	0.98 ± 0.06	1.00 ± 0.05	1.39 ± 0.08^{aa}	1.19 ± 0.05	1.38 ± 0.07^{a}	1.64 ± 0.03^{aaab}	1.96 ± 0.09^{aaabbb}	2.37 ± 0.18$^{aaabbb***¤}$
	CXC subfamily	*CxCl10*	1.07 ± 0.17	1.02 ± 0.11	1.71 ± 0.29	2.25 ± 0.14^{a}	3.30 ± 0.24*	3.77 ± 0.44**	3.73 ± 0.42^{aaabb}	51.19 ± 1.14^{aaabbb***}	98.22 ± 5.83$^{aaabbb***¤¤¤}$
Pro-inflammatory cytokines		*Il1b*	1.05 ± 0.15	0.76 ± 0.05	0.95 ± 0.04	1.74 ± 0.21	1.98 ± 0.28^{aa}	2.00 ± 0.32	2.52 ± 0.32^{aa}	3.59 ± 0.20^{aaabbb}	8.96 ± 2.04$^{aaabb**¤}$
	Hematopoietins	*Il6*	1.07 ± 0.14	1.68 ± 0.12**	1.59 ± 0.06*	3.30 ± 0.21^{aaa}	3.30 ± 0.41	4.32 ± 0.31^{a}	5.44 ± 0.45^{aaabbb}	7.52 ± 1.00^{aaabbb}	10.59 ± 1.10^{aaabbb**}
		Il6st	1.00 ± 0.04	1.04 ± 0.03	0.96 ± 0.04	1.15 ± 0.03^{aa}	1.28 ± 0.04^{aa*}	1.18 ± 0.04^{a}	1.23 ± 0.02^{aaa}	1.18 ± 0.06	1.26 ± 0.08^{aa}
	TNF family	*Tnfα*	1.01 ± 0.07	2.00 ± 0.17**	0.98 ± 0.08$^{¤¤¤}$	1.22 ± 0.12	1.57 ± 0.15	1.98 ± 0.11**	2.87 ± 0.32^{aaabbb}	3.19 ± 0.31^{aabbb}	5.50 ± 0.82$^{aaabbb**¤}$
		Tnfrsf1a	1.02 ± 0.08	1.12 ± 0.06	1.15 ± 0.05	1.34 ± 0.08^{a}	1.37 ± 0.05	1.22 ± 0.03	1.25 ± 0.06	1.38 ± 0.11	1.45 ± 0.13^{a}
Anti-inflammatory cytokines	IL-10 family	*Il10*	1.03 ± 0.11	1.36 ± 0.11	0.83 ± 0.12$^{¤}$	0.66 ± 0.08	0.83 ± 0.10	1.08 ± 0.17	1.11 ± 0.14	1.20 ± 0.26	2.02 ± 0.37^{a}
		Il10ra	1.01 ± 0.04	0.92 ± 0.03	1.12 ± 0.05$^{¤}$	1.19 ± 0.07^{a}	1.24 ± 0.04^{aaa}	1.00 ± 0.05$^{¤}$	1.22 ± 0.03^{a}	1.30 ± 0.07^{aaa}	1.64 ± 0.15$^{aabbb**¤}$
		Il10rb	1.01 ± 0.05	0.96 ± 0.05	1.06 ± 0.03	1.57 ± 0.15^{aaa}	1.68 ± 0.09^{aaa}	1.51 ± 0.04^{aaa}	1.64 ± 0.04^{aaa}	1.63 ± 0.09^{aaa}	1.84 ± 0.10^{aaabb}
	TGF beta family	*Tgfb1*	1.01 ± 0.05	1.01 ± 0.02	0.98 ± 0.04	0.91 ± 0.04	0.90 ± 0.02	0.86 ± 0.03	0.82 ± 0.05^{a}	0.89 ± 0.08	1.10 ± 0.09^{b}
		Tgfb2	1.01 ± 0.06	1.05 ± 0.01	1.03 ± 0.04	1.08 ± 0.03	1.11 ± 0.03	1.01 ± 0.04	1.10 ± 0.04	1.01 ± 0.05	1.01 ± 0.08

* $p < 0.05$,

** $p < 0.01$,

*** $p < 0.001$ *Epm2a*$^{-/-}$ or *Epm2b*$^{-/-}$ compared with age-matched WT,

$^{\square}$ $p < 0.05$,

$^{\square\square}$ $p < 0.01$,

$^{\square\square\square}$ $p < 0.001$ *Epm2b*$^{-/-}$ compared with *Epm2a*$^{-/-}$,

^{a} $p < 0.05$,

^{aa} $p < 0.01$,

^{aaa} $p < 0.001$ compared with animals aged 16 days,

^{b} $p < 0.05$,

^{bb} $p < 0.01$,

^{bbb} $p < 0.001$ compared with animals aged 3 months.